Research Article | Vol. 11, No. 8 / 1 August 2021 / Optical Materials Express 2639
Optical Materials EXPRESS

Photonic lanterns: a practical guide to filament tapering

JOHN J. DAVENPORT,* MOMEN DIAB, PRANAB J. DEKA, AASHANA TRIPATHI, KALAGA MADHAV, AND MARTIN M. ROTH

Leibniz-Institut für Astrophysik Potsdam, An der Sternwarte 16, D-14482 Potsdam, Germany
*jdavenport@aip.de

Abstract: We present a detailed method of tapering and drawing photonic lanterns using a filament glass processing system. Single-mode fibers (SMFs) were stacked inside a low refractive index, fluorine-doped capillary, which was then heated and tapered to produce a transition from single-mode to multi-mode. Fabrication parameters were considered in four categories: method of preparation and stacking of SMFs into a capillary, heat and filament dimensions of the glass processor, capillary ID, and the use of vacuum during tapering. 19- and 37- fiber lanterns were drawn, demonstrating good fusion between SMF claddings, a clear differentiation between core and cladding in the multimode (MM) section, and well-ordered arrangements between SMFs, which is controlled during the tapering process. The transmission efficiency of a 19-fiber photonic lantern, compared to an MMF with the same core diameter and NA, has a relative transmission efficiency of 1.19 dB or 67.1%. The steps and parameters provided in this paper form a framework for fabricating quality photonic lanterns.

1. Introduction

A new era began in the field of astrophotonics with the invention of the photonic lantern (PL), an optical device that couples light from a multi-mode fiber (MMF) to many single mode fibers (SMFs) and vice versa [1,2,3,4,5]. Among other applications, PLs have been shown to exhibit excellent light scrambling properties [6,7] modal noise reduction [7,8], facilitate OH line filtering [9,10,11] and coupling to single-mode photonic chips. A common form of PL consists of a stack of SMFs tapered and fused together to form a single MMF. Light couples between the SMFs and the MM section via a gradual adiabatic taper transition [4].

Common methods of manufacturing PLs include SMF tapering [3,6,12,13], tapering multi-core fibers [7,8], and ultrafast laser inscription (ULI) [14,15]. The first method involves inserting or 'stacking' a bundle of SMFs into a low-index glass capillary, then applying heat and tension to taper it down to form the MMF section. The claddings of the SMFs fuse together to form the core of the MMF section, while the capillary becomes the new cladding. Noordegraaf et. al. [16] produced a 19 fiber PL by this method which was fusion spliced to a 50 µm core MMF, achieving a transmission efficiency of 1.1 dB. Yerolatsitis et. al. produced a 7 fiber PL for use as a pseudoslit, with an SMF to MMF transmission efficiency of 0.9 dB [17]. Earlier, Noodegraaf et. al. (2010) produced a large PL with 61 fibers, demonstrating a transmission efficiency of 0.76 dB.

The quality and performance of the fabricated PL depend strongly on parameters such as the size and number of SMFs, material and dimensions of capillary, the temperature and tension applied during tapering, method of preparation and stacking of SMFs, and the use of vacuum. However, there is no guide to date that describes the influence of the parameters on the quality of PLs. In this paper, we fabricate PLs of 19 and 37 fibers by heating and tapering, using a Vytran GPX-3000 filament glass processing system, and the method was optimized extensively. We present a detailed description of what was considered in this optimization.

#427903 https://doi.org/10.1364/OME.427903
Journal © 2021 Received 16 Apr 2021; revised 25 Jun 2021; accepted 26 Jun 2021; published 20 Jul 2021

Optical Materials EXPRESS

2. Theory

Figure 1 shows a diagram of the type of PL used in this study. It consists of an SMF region, a transition region and an MMF region with a series of SMFs. Although bidirectional adiabatic propagation is possible in such a device, here we will be focusing on light propagation from the MM region to the SM region.

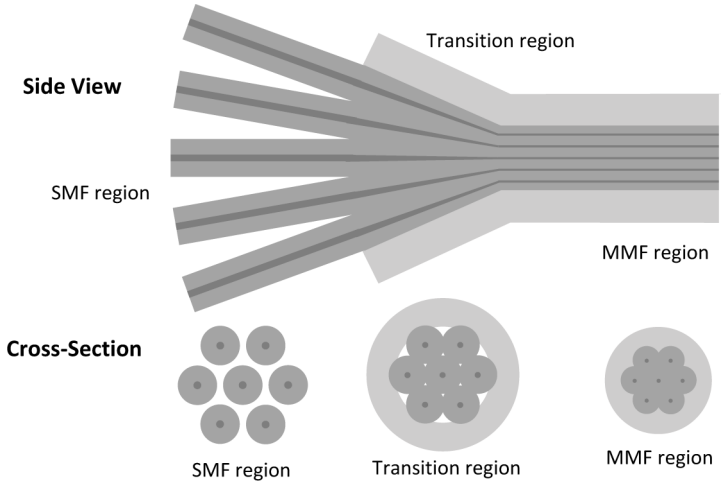

Fig. 1. Diagram of a typical PL, in side view and cross-section.

The MMF region is formed by fusing and tapering a stack of SMFs bundled inside a capillary. The claddings of the SMFs fuse and form the core of the MMF, with the outer capillary forming the cladding of the MMF region. It is therefore necessary that the refractive indices of the SMF cores n_1, the SMF cladding n_2, and the capillary n_3 must be:

$$n_1 > n_2 > n_3 \tag{1}$$

Above the cut-off wavelengths of the individual fibers, the propagation characteristics of the SMFs are preserved in the SMF region. However, at the transition region, where the cores of the individual SMFs are tapered down into smaller diameters, the mode can no longer be contained, and is coupled out into the surrounding cladding material. The residuals of the SMF cores remain present in the MM section but after tapering should be too narrow to effectively couple light within the design wavelength band.

For light to be able to transition adiabatically, the number of optical modes supported by the SM region (N_{sm}) should be equal to or greater than the number supported by the MM region [2]. The approximate number of unpolarized modes supported within an MMF is given by [18]:

$$N_{mm} \approx \left(\frac{V_{mm}}{2}\right)^2 = \left(\frac{\pi d_{mm} NA_{mm}}{2\lambda}\right)^2, \tag{2}$$

where V_{mm} is the V-parameter for the fiber equal to $(\pi d_{mm} NA_{mm})/\lambda$ [4], d_{mm} is the diameter of the fiber core, NA_{mm} is the numerical aperture and λ is the wavelength. Assuming all the cores in the SM region support a single, unpolarized mode, the number of modes supported by the SM region, N_{sm}, is equal to the number of SMFs. However, it is not uncommon for PLs to be produced with MMFs larger than this condition as a tradeoff between efficiency and avoiding very thin fibers that are difficult to handle [3].

The arrangement of fibers is also important for efficient coupling between the MM and SM regions. Ideally, the modes supported by the MM region should match the supermodes supported

Optical Materials EXPRESS

by the SM region [4]. It was considered that the greater the density of cores at the start of the SM region, and the smaller the gaps between them, the more likely it was that a given mode be matched. The taper transition length is defined as the length of the fiber between the SMF and the MMF sections. This taper rate is critical for PLs when light propagates from SMFs to MMF: a high taper rate can result in light leaking out of the transition region into the surrounding capillary to become cladding modes [4]. Adiabatic taper length (L) scales approximately with $L \propto N_{sm}{}^2$ [13]. Less has been written about transitions in the MMF to SMF direction. In this paper, it was ensured that taper angles did not exceed that of the numerical aperture of the MM region to prevent the transition region being under-filled.

3. Method

Table 1 lists the specifications of the SMFs and capillaries used in fabricating PLs. Florine-doped capillaries manufactured and provided by T. A. Birks, Centre for Photonics and Photonic Materials, University of Bath, were used to provide a lower refractive index cladding (n_3) for the MM section. The PLs described in this paper use reduced-clad SMFs with lower than usual cladding diameters, 80 μm. With reduced clad fibers, a higher number of SMFs can be stacked inside capillaries. Two kinds of SMF were used in order to control mode coupling in the PLs, which is outside the scope of this paper.

Table 1. Specification of SMFs and capillaries used for this paper

Capillary	OD μm	ID μm	Index at 1550 nm
Bath University F-doped 900	913	645	1.440
Bath University F-doped 620	628	435	1.427
Fiberware CAP 405/1000; F300	1000	400	1.444
SMF	Diameter μm	Wavelength nm	NA
Newport F-SM1500-6.4/80	80	1550-1650	0.13
Newport F-SM1500-9/80	80	1310-1550	0.15 - 0.17
Newport F-SMF-28	125	1310-1550	0.14

Figure 2 shows a diagram of a typical stack. Stacks were then drawn and fused using a GPX-3000 Vytran glass processing system. By applying tension and heat from a tungsten filament, the cores and claddings of the SMFs could be tapered down to form the core of an MMF, with the surrounding capillary forming the MMF cladding. When the capillary ID is at or close to the minimum needed to contain them, SMFs will take a close-packed and predictable arrangement referred to as "optimal". These arrangements depend on the number of SMFs present [19].

Figure 3 shows micrographs of a 19 fiber PL at different stages of tapering. Individual SMFs can be seen stacked inside the capillary before tapering. In the early taper region, dark lines show where air-gaps exist between the SMFs, which thin and disappear along the taper. In the late taper region, it can be seen that the SMFs have fully fused and no more air gaps remain. The lighter lines are the residual cores of the SMFs. Last is the newly formed MMF region.

Table 2 gives a step by step procedure for producing PLs. The parameters identified as important for fabricating PLs fell into four categories: preparation and stacking of SMFs into a capillary; settings of the glass processor unit such as filament size and power; capillary internal diameter (ID); and the use of a vacuum during tapering. These parameters are discussed in detail below. Examples of the parameters used in practice for the PLs used in this paper can be found in Table 3 in the results section.

Optical Materials EXPRESS

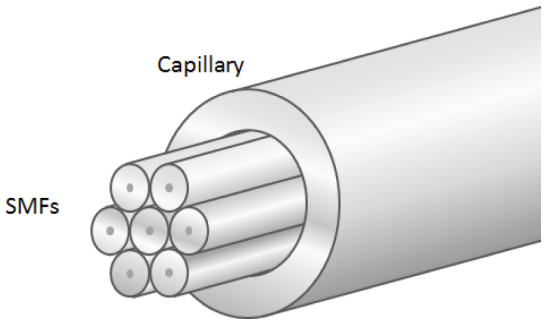

Fig. 2. Diagram of a typical SMF stack inside a glass capillary. The acrylate jacket of SMFs is stripped before inserting into the capillary.

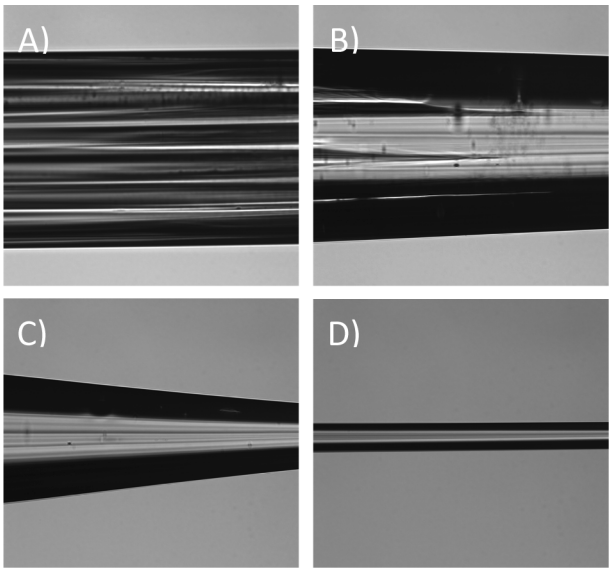

Fig. 3. Micrographs of various stages of tapering of a 19 fiber PL. A) Untapered SMFs stacked inside the capillary. B) Early transition region, showing SMFs starting to fuse. C) Late transition region with fully fused SMFs. D) MMF region.

Table 2. Procedure for producing PLs

1	Pre-taper capillary to give appropriate ID. Keep attached undrawn section
2	Strip and clean SMFs
3	Stack SMFs into capillary
4	Run stacked capillary through filament x 3 for collapse
5	Draw and taper stacked capillary to form PL

Optical Materials EXPRESS

Table 3. Parameters used to produce the 19 fiber and 37 fiber PLs described above

19 fiber PL	
Capillary	Bath University F-doped 620
Reduced capillary	OD 574, ID 393
SMFs	Newport F-SM1500-6.4/80
Filament	FTAT2[a]
Power	130 W
Vacuum	Yes
37 fiber PL	
Capillary	Bath University F-doped 900
Reduced capillary	OD 785, ID 555
SMFs	Newport F-SM1500-6.4/80
Filament	FTAT3
Power	175 W
Vacuum	Yes

[a]FTAV2 filament also suitable.

3.1. Preparation and stacking of SMFs

Before inserting the SMFs into the capillaries, it was necessary to remove jackets and clean the SMFs. Coatings were removed using a room temperature bath of dichloromethane (CH_2Cl_2). The fibers were then wiped with a lint free tissue soaked in acetone ($(CH_3)_2CO$), followed by Isopropyl alcohol (IPA) ($CH_3CHOHCH_3$). The capillaries were flushed and cleaned with acetone and IPA as well. It is important to ensure that there is no dirt or grease on the SMFs and capillary, both to avoid contamination and because any burnable materials left in the stack may damage it or introduce inhomogeneities during the tapering process.

In order to achieve uniform packing, the SMFs must fit tightly within the capillary. The capillaries used in this work were acquired with a diameter higher than was needed and drawn down before use. This was found to be useful when inserting SMF bundles as an undrawn section could be left attached, the larger internal diameter of which helped to guide SMFs. The SMFs were dipped in IPA, and the surface tension pulled the individual fibers close into a roughly circular arrangement. The capillary itself was flooded with IPA to reduce friction between the SMFs and the capillary wall. Once inserted, a vacuum pump was used to remove any excess IPA before applying heat. Figure 4 shows a photograph of SMFs stacked into a capillary ready for tapering.

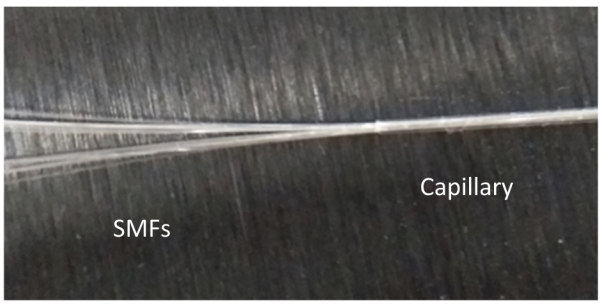

Fig. 4. Photograph of SMFs (left) stacked into a capillary (right).

Optical Materials EXPRESS

3.2. Glass processor unit settings

Important settings of the glass processor unit included filament type and size, the power used to heat the capillary and fibers, and tension applied during the process. These settings depend on the specifics of the diameters and materials used for the PL, which are described in the operating manual of the glass processing system, but there are a few points worth discussing.

Fluorine-doped silica glass becomes viscus at a lower temperature than un-doped glass, varying with fluorine concentration. The temperature was dependent on the filament power, and it was found that too high a power resulted in a lower than intended capillary diameter. 100 W filament power was optimum for the capillaries used in this work, but other capillaries may require a different power. It is recommended that a number of test tapers are drawn, and their resulting diameters be compared to the target diameter, to find the optimum filament power. Before tapering the PL, the stacked capillary was first run through the heated filament three times to collapse the capillary and the SMFs together and decrease the chance of slipping between different components when tension is applied. A filament power of 100 W was typically used for this step.

Tension was monitored during the tapering process using the glass processor unit inbuilt tension monitor. An initial tension of 20 g was applied by moving one of the holding blocks before starting. Figure 5 shows the ideal tension variation during the automatic tapering and drawing process of a PL, as suggested in private discussions with the manufacturer. Tension starts at 20 g, then drops to zero when the filament heats up. The holding blocks then move, increasing the tension to roughly 200–300 g. As the stacked capillary starts to stretch, the tension decreases, dropping to around 20 g for the duration of the draw process. Finally, the tension drops to zero as the process completes. While this variation is not exact, significant deviations from it may indicate problems with the process. Figure 6 shows some examples.

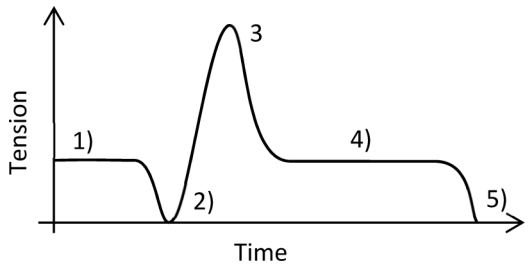

Fig. 5. Diagram of ideal tension variation during taper and draw process, 1) initial 20 g, 2) 0 g as the filament heats up, 3) 200–300 g as tension applies, 4) ≈20 g as stack stretches, decreasing tension, 5) drops to zero as process finishes. Not to scale.

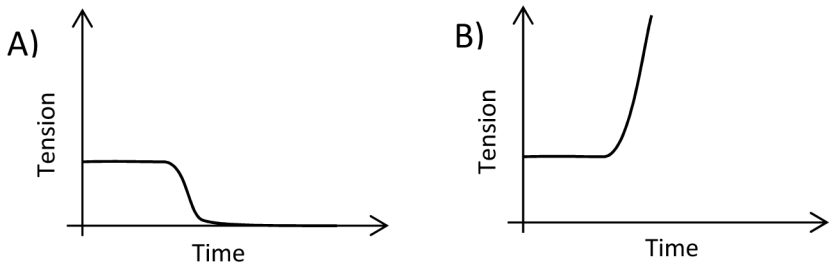

Fig. 6. Examples of tension indicating problems. A) Temperature much too high. B) Temperature too low or, counter intuitively, slightly too high. Both diagrams are not to scale.

Optical Materials EXPRESS

3.3. Capillary ID

The ID of the capillary is important for ensuring a regular packing between SMFs with the minimum space. Figure 7 shows two micrograph cross-sections of 37 SMF transition regions with different initial capillary IDs. In A), 575 μm, there are significant air gaps shown in black between SMFs, and they have not fused together well. In B), 560 μm, the tight fit of the capillary has forced the SMFs into a close packed, regular pattern. At this point in the transition region they have partially fused, the much smaller air gaps will disappear before reaching the MMF region (Fig. 3).

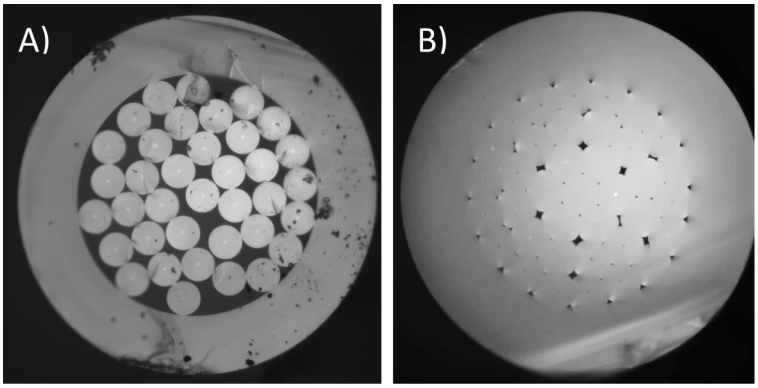

Fig. 7. Micrograph cross-sections of the 37 SMF transition regions, from different capillary IDs. A) Pre-taper ID of 575 μm is too large, leading to disordered SMFs. B) Pre-taper ID of 560 μm forces SMFs into an ordered pattern.

Note that the B) does not follow an exact hexagonal pattern, the outer ring being closer to a circle than a hexagon. This is because, while hexagonal packing is the most efficient packing within unbounded space, this pattern fits better into a circular capillary. This is described in more detail in Davenport et. al. [19], and has been demonstrated to work up to at least 61 cores by Noordegraaf et. al. [12,20]. To achieve the desired IDs, capillaries were drawn to a smaller diameter using the glass processing unit. This had the added advantage of shaping the capillary as a funnel, into which the SMF bundle could be inserted more easily.

3.4. Vacuum during tapering

Even when the SMFs inside the capillary are efficiently packed, air gaps remain between them and between the capillary walls. It is necessary that these air gaps are removed during the taper or they will interfere with the propagation of light within the MMF section of the PL. A vacuum pump (Linicon LV-125A) was therefore connected to one end of the capillary during the tapering process, to remove air bubbles and allow unimpeded fusion to occur between SMFs and to the capillary.

Figure 8 shows micrographs of two PLs cleaved in the MMF section, drawn with vacuum and one without. The dark sections seen in A) are air bubbles. Note that the other end of the capillary does not need to be sealed during tapering, the decreased pressure created by the vacuum pump is sufficient to avoid air bubbles.

Optical Materials EXPRESS

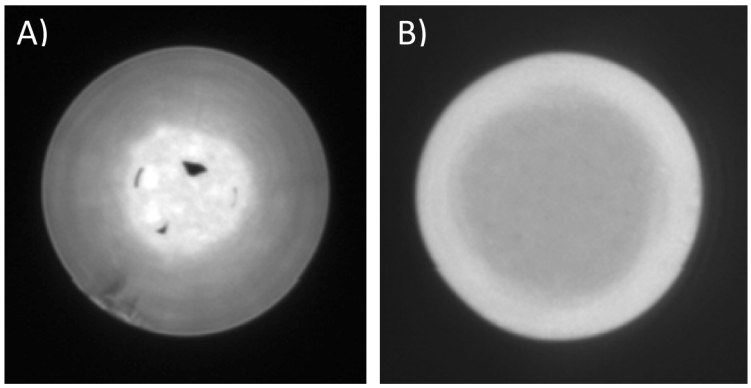

Fig. 8. Micrograph cross-sections of two MMF sections, A) No vacuum (19 fibers, pre-taper SMF diameter 125 μm, capillary ID 400 μm), B) vacuum applied (19 fibers, pre-taper SMF diameter 125 μm, capillary ID 675 μm).

4. Results

Here we present details of several PLs produced by the above method. Table 3 shows a list of parameters used to produce 19 fiber and 37 fiber PLs.

Figure 9 shows micrographs of a 19 fiber PL cleaved at the transition region and the MMF region. In the transition region it can be seen that the claddings of the SMFs have fused together. The SMF cores can be seen in the center of each fiber, some illuminated and some not based on the particular paths that the side-illuminated light took through the assembly. Fibers have taken on a regular arrangement of two concentric rings around a central SMF, enforced by the internal diameter of the capillary. In the MMF region, it can be seen that light is confined within the new 'core' of the MMF, surrounded by the cladding that is the capillary. The residual cores are still visible, too small to efficiently confine light, but continue to have a perturbative effect on the light around them indicated by the bright points. The positions of these points, where visible, indicate that the regular arrangement of SMFs has been maintained through the fusing process.

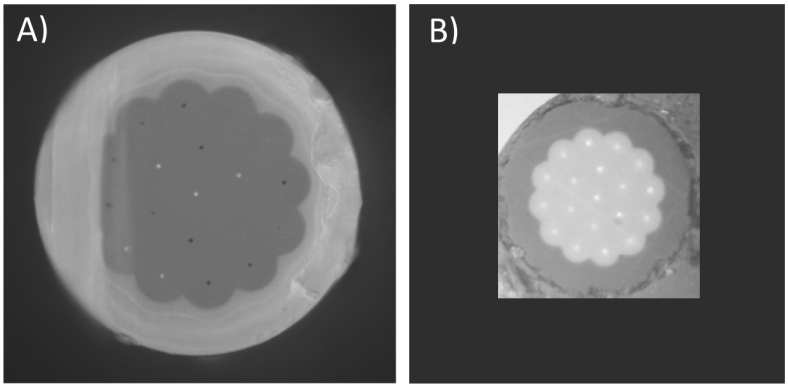

Fig. 9. Micrographs of cleaved cross-sections of a 19 fiber PL. A) Transition region, illuminated from the side. B) MMF section illuminated from the end. Taper ration: 7.4. Taper length 5 mm.

Figure 10 shows micrographs of a 37 fiber PL, cleaved at the MMF region. It can again be seen that light is confined within the new core, and SMFs have taken on a regular pattern of three

Optical Materials EXPRESS

concentric rings around a central SMF. Similarly to the 19 fiber PL, the brighter points of the residual cores can be seen, and show that the regular arrangement has been maintained.

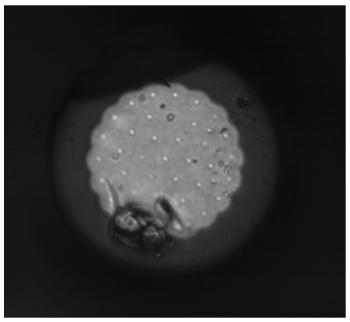

Fig. 10. Micrographs of cleaved cross-sections of 37 fiber PLs. MMF section illuminated from the end. Cleave damage is also shown. Taper ration: 15.0. Taper length 5 mm. The MMF surface was damaged during cleaving, but the shape of the core and cladding can still be seen.

Figure 11 shows the refractive index profiles of the MMF section of a 19 and a 37 fiber PL, taken with a refractive index profiler (Interfiber Analysis IFA-100 multipwavelength Optical Fiber Analyser). In this case the 19 fiber PL was drawn to give a core of 50 µm in order to compare to the MMF mentioned below. The 37 fiber PL was drawn to a smaller size to test the limits of the system. Different taper ratios can be achieved by varying the speeds of the holding blocks.

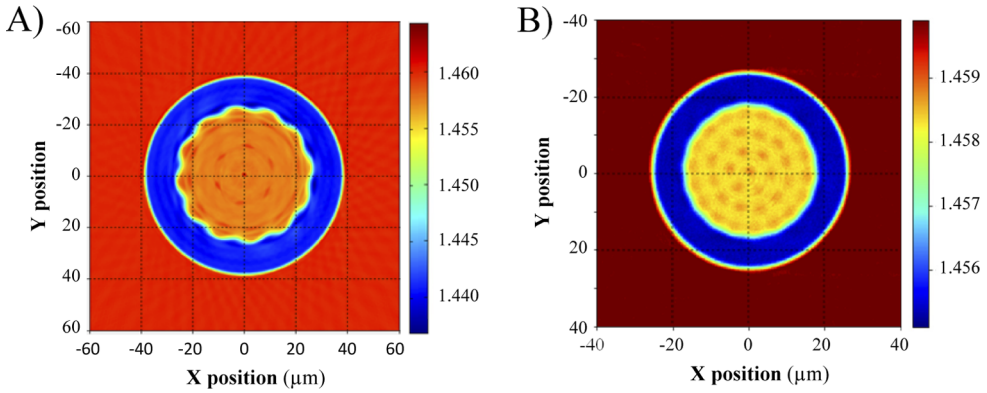

Fig. 11. Refractive index profile of A) a 19 and B) a 37 fiber PL, MMF section. The low refractive index capillaries formed the claddings of the MMF (blue), the claddings of the SMFs fused to become the cores of the MMFs (A) orange, B) yellow), and the residual cores of the SMFs show an ordered pattern (A) red, B) orange).

In both cases it can be seen that the lower refractive index capillaries surround the fibers forming claddings, and the claddings of the SMF fibers have fused together to form MMF core regions. The residual cores of the SMFs can be seen inside the MMF core regions, showing ordered arrangements, demonstrating that the order seen in Fig. 10 is maintained through the tapering process. The red/orange dots representing the residual cores are significantly larger than the cores themselves (calculated to be approximately 440 nm) due to the diffraction limit of the 633 nm light used in the measurement.

Next, the transmission of a 19 fiber PL was measured in the MMF to SMF direction. SMFs used were 14 F-SM1500-6.4/80 and 5 F-SM1500-9/80, inside an F-doped 620 capillary. It

Optical Materials EXPRESS

was tapered, with parameters given in Table 3, to a 50 µm MMF core diameter and 0.22 NA at 1550 nm. A diameter larger than the mode-matching condition was chosen (Eq. (2)) to allow a cladding diameter of 78 µm, large enough to be practically handled, and to allow an effective comparison to be made with a 50 µm core MMF.

Light from a 1550 nm laser diode (45 mW, QDFBLD-1550-50N, QPhotonics LLC) was coupled into the MMF end, overfilling the angular aperture. Output light was then measured using an integrating sphere (25.4 mm diameter sphere, InGaAs photodiode, S144C, Thorlabs). In order to isolate the transmission efficiency of the PL from effects such as coupling efficiency into the device, transmission was tested with an MMF patch cable with the same core diameter and NA under the same conditions (core diameter 50 µm, NA 0.22, M14L02, Thorlabs) . This gave a transmission efficiency of the PL of $67.1 \pm 0.6\%$. This compares well to PLs produced by other groups.

5. Conclusions

A common method for producing PLs is to apply heat and tension to a capillary containing a stack of SMF, tapering the stack such that SMFs fuse into a single MMF core. This paper presents parameters that should be taken into account, outlines a method, and characterizes a 37 PL produced using optimum fabrication settings.

Parameters considered included preparation and stacking of SMFs into a capillary, settings of the glass processor unit, capillary ID, and the use of vacuum during tapering. A 37 fiber PL and a 19 fiber PL were demonstrated, where the claddings of the SMFs were demonstrated to fuse into a single, solid core at the MMF section, and a clear differentiation between this core and the MMF cladding formed by the capillary. Order was observed in the fiber arrangements, enforced by matching the capillary internal diameters with the fiber stacks, and this order was maintained during tapering process.

The results demonstrate the production of PLs with clearly defined SMF and MMF sections. During tapering, MMF cores formed from fused SMF claddings, maintaining the order enforced during stacking. The transmission efficiency of a 19 fiber PL was measured relative to a MM patch cable with the same core diameter and NA, finding a relative transmission efficiency of $67.1 \pm 0.6\%$, comparing well to similar devices produced by other groups.

It is hoped that this paper can be used as a resource for researchers wishing to draw their own PLs. Optimum parameters will differ depending on the desired PL being drawn, and researchers must experiment to find which are appropriate for the situation. However, this paper presents which parameters are important to consider, and how the optimum parameters can be found.

Funding. Deutsche Forschungsgemeinschaft (326946494); Horizon 2020 Framework Programme (730890).

Acknowledgments. Horizon 2020: This project has received funding from the European Union's Horizon 2020 research and innovation programme under grant agreement No 730890. This material reflects only the author's views and the Commission is not liable for any use that may be made of the information contained therein.

This work was supported by the Deutsche Forschungsgemeinschaft (DFG) through project 326946494, 'Novel Astronomical Instrumentation through photonic Reformatting'.

Disclosures. The authors declare that there are no conflicts of interest related to this article.

Data availability. Data underlying the results presented in this paper are not publicly available at this time but may be obtained from the authors upon reasonable request.

References

1. S. G. Leon-Saval, T. A. Birks, N. Y. Joly, A. K. George, W. J. Wadsworth, G. Kakarantzas, and P. S. J. Russell, "Splice-free interfacing of photonic crystal fibers," Opt. Lett. **30**(13), 1629–1631 (2005).
2. S. G. Leon-Saval, A. Argyros, and J. Bland-Hawthorn, "Photonic lanterns: a study of light propagation in multimode to single-mode converters," Opt. Express **18**(8), 8430–8439 (2010).
3. D. Noordegraaf, P. M. W. Skovgaard, M. D. Nielsen, and J. Bland-Hawthorn, "Efficient multi-mode to single-mode coupling in a photonic lantern," Opt. Express **17**(3), 1988–1994 (2009).

Optical Materials EXPRESS

4. T. A. Birks, I. Gris-Sánchez, S. Yerolatsitis, S. G. Leon-Saval, and R. R. Thomson, "The photonic lantern," Adv. Opt. Photonics **7**(2), 107–167 (2015).
5. N. M. Mathew, L. Grüner-Nielsen, M. A. U. Castaneda, and K. Rottwitt, "A novel fabrication method for photonic lanterns," *Optical Fiber Communication Conference (2018)*, paper M4D.4, Optical Society of America (2018).
6. T. A. Birks, B. J. Mangan, A. Díez, J. L. Cruz, and D. F. Murphy, "'Photonic lantern' spectral filters in multi-core fiber," Opt. Express **20**(13), 13996–14008 (2012).
7. I. Gris-Sánchez, D. M. Haynes, K. Ehrlich, R. Haynes, and T. A. Birks, "Multicore fiber photonic lanterns for precision radial velocity science," Mon. Not. R. Astron. Soc. **475**(3), 3065–3075 (2017).
8. D. M. Haynes, I. Gris-Sánchez, T. A. Birks, and R. Haynes, "Optical fiber modal noise suppression in the NIR region using multicore fiber and photonic lanterns," *Advances in Optical and Mechanical Technologies for Telescopes and Instrumentation III*, R. Geyl and R. Navarro, eds., 214, SPIE (2018).
9. J. Baudrand and G. A. H. Walker, "Modal noise in high-resolution, fiber-fed spectra: a study and simple cure," Publ. Astron. Soc. Pac. **113**(785), 851–858 (2001).
10. J. Bland-Hawthorn, M. Englund, and G. Edvell, "New approach to atmospheric OH suppression using an aperiodic fiber Bragg grating," Opt. Express **12**(24), 5902–5909 (2004).
11. C. Q. Trinh, S. C. Ellis, J. Bland-Hawthorn, J. S. Lawrence, A. J. Horton, S. G. Leon-Saval, K. Shortridge, J. Bryant, S. Case, M. Colless, W. Couch, K. Freeman, H. G. Löhmannsröben, L. Gers, K. Glazebrook, R. Haynes, S. Lee, J. O'Byrne, S. Miziarski, M. M. Roth, B. Schmidt, C. G. Tinney, and J. Zheng, "GNOSIS: the first instrument to use fiber Bragg gratings for OH suppression," Astron. J. **145**(2), 51–63 (2013).
12. D. Noordegraaf, P. M. W. Skovgaard, M. D. Maack, J. Bland-Hawthorn, R. Haynes, and J. Lægsgaard, "Multi-mode to single-mode conversion in a 61 port photonic lantern," Opt. Express **18**(5), 4673–4678 (2010).
13. S. Yerolatsitis, I. Gris-Sánchez, and T. A. Birks, "Adiabatically-tapered fiber mode multiplexers," Opt. Express **22**(1), 608–617 (2014).
14. R. J. Harris, D. G. MacLachlan, D. Choudhury, T. J. Morris, E. Gendron, A. G. Basden, G. Brown, J. R. Allington-Smith, and R. R. Thomson, "Photonic spatial reformatting of stellar light for diffraction-limited spectroscopy," Mon. Not. R. Astron. Soc. **450**(1), 428–434 (2015).
15. R. R. Thomson, T. A. Birks, S. G. Leon-Saval, A. K. Kar, and J. Bland-Hawthorn, "Ultrafast laser inscription of an integrated photonic lantern," Opt. Express **19**(6), 5698 (2011).
16. D. Noordegraaf, P. M. W. Skovgaard, R. H. Sandberg, M. D. Maack, J. Bland-Hawthorn, J. S. Lawrence, and J. Lægsgaard, "Nineteen-port photonic lantern with multimode delivery fiber," Opt. Lett. **37**(4), 452 (2012).
17. S. Yerolatsitis, K. Harrington, and T. A. Birks, "All-fiber pseudo-slit reformatters," Opt. Express **25**(16), 18713–18721 (2017).
18. S. G. Leon-Saval, A. Argyros, and J. Bland-Hawthorn, "Photonic lanterns," Nanophotonics **2**(5-6), 429–440 (2013).
19. J. J. Davenport, M. Diab, K. Madhav, and M. M. Roth, "Optimal SMF packing in photonic lanterns: comparing theoretical topology to practical packing arrangements," J. Opt. Soc. Am. B **38**(7), A7–A14 (2021).
20. D. Noordegraaf, P. M. W. Skovgaard, M. D. Maack, J. Bland-Hawthorn, R. Haynes, and J. Lægsgaard, "Efficient multi-mode to single-mode conversion in a 61 port photonic lantern," *Fiber Lasers VII: Technology, Systems, and Applications* 7580, 75802D, International Society for Optics and Photonics (2010).